Geoscience Frontiers 9 (2018) 967–975

HOSTED BY

Contents lists available at ScienceDirect

China University of Geosciences (Beijing)

Geoscience Frontiers

journal homepage: www.elsevier.com/locate/gsf

Research Paper

Exploring the metamorphic consequences of secular change in the siliciclastic compositions of continental margins

Gautier Nicoli [a,*], Brendan Dyck [a,b,1]

[a] Department of Earth Sciences, University of Cambridge, Cambridge CB2 3EQ, UK
[b] Department of Earth Sciences, Simon Fraser University, Burnaby, British Columbia V5A 1S6, Canada

ARTICLE INFO

Article history:
Received 1 July 2017
Received in revised form
10 November 2017
Accepted 6 December 2017
Available online 3 January 2018

Keywords:
Secular change
Shale
Greywacke
Dehydration melting
Thermodynamic modelling
Perple_X

ABSTRACT

Shale and greywacke compositions from the Archean to Phanerozoic record a secular change in the siliciclastic material that comprises much of Earth's continental margins, past and present. This study explores the metamorphic consequence of these compositional changes, by comparing phase equilibrium models constructed for average Archean, Proterozoic, and Phanerozoic shale and greywacke compositions equilibrated along two Barrovian-type geotherms: 1330 °C/GPa (A) and 800 °C/GPa (B). Our models show that Archean siliciclastic rocks can retain up to 4 vol.% water at middle to lower crustal conditions, nearly twice that of Proterozoic and Phanerozoic compositions. The increased ferromagnesium content of Archean siliciclastic rocks stabilizes chlorite to higher temperatures and results in a biotite-rich assemblage at solidus temperatures. Accordingly, water-absent biotite dehydration melting is predicted to play a greater role in the generation of melt in the metamorphism of Archean aged units, and water-absent muscovite dehydration melting is of increasing importance through the Proterozoic and Phanerozoic. This secular variation in predicted mineral assemblages demonstrates the care with which metamorphic facies diagrams should be applied to Archean compositions. Moreover, secular changes in the composition of shale and greywacke is reflected in the evolution of anatectic melt towards an increasingly less viscous, Ca-rich, and Mg-poor monzogranite.

© 2018, China University of Geosciences (Beijing) and Peking University. Production and hosting by Elsevier B.V. This is an open access article under the CC BY-NC-ND license (http://creativecommons.org/licenses/by-nc-nd/4.0/).

1. Introduction

Evolution of the continental lithosphere composition is echoed in secular compositional changes of supracrustal rocks, which are an archive that can be used to understand and quantify geological processes through Earth's history (e.g. Engel et al., 1974; McLennan, 1982, 2001; McLennan and Taylor, 1991; Condie, 1993; Rudnick, 1995; Veizer and Mackenzie, 2003). The 3.0–2.5 Ga transition between the Neoarchean and Proterozoic marks an important period during which sediments underwent significant compositional changes. Archean sediments are generally more ferromagnesium-rich (i.e. total Mg + Fe) compared with Proterozoic and Phanerozoic sediments (Condie, 1993). These changes are generally interpreted to be the consequences of the progressive onset of modern-like plate tectonics (e.g. Dhuime et al., 2012; Dyck et al., 2015; Nicoli et al., 2016; Palin and White, 2016); continental growth and increase in the amount of subaerial land mass (Flament et al., 2013; Dhuime et al., 2017); and changes in atmospheric conditions (*i.e.* chemical weathering, surface oxidation) (Condie, 1993; Johnsson, 1993; Barley et al., 2005; Campbell and Allen, 2008). The presence of shale (or pelite) and greywacke in the sedimentary record can be tracked back to ca. 3.5 Ga (Veizer and Mackenzie, 2003). When metamorphosed, these two lithologies commonly comprise mineral assemblages dominated by water-rich minerals such as biotite, muscovite, staurolite and amphibole. Accordingly, they represent important crustal water reservoirs which, when buried within collisional orogenic settings, may exert an important control on melt fertility, and mass transfer (e.g. Clemens and Vielzeuf, 1987; Le Breton and Thompson, 1988; Douce and Johnston, 1991; Stevens et al., 1997; Sawyer et al., 2011; Nicoli et al., 2017). Variation in the amount of mineral-bound water may have profound impact on the rheology of the crust (e.g. Kolb, 2008), metamorphic fluid production (Walther and Orville, 1982; Ague, 2011), as well as the thermal state of the crust (e.g. Stüwe, 1995; Depine et al., 2008).

In this study, we focus on the equilibrium assemblages of buried and metamorphosed shale and greywacke in an orogenic setting.

* Corresponding author.
E-mail addresses: ng422@cam.ac.uk (G. Nicoli), brendan_dyck@sfu.ca (B. Dyck).
[1] Present address: Department of Earth Sciences, Simon Fraser University, Burnaby V5A 1S6, Canada
Peer-review under responsibility of China University of Geosciences (Beijing).

https://doi.org/10.1016/j.gsf.2017.12.009
1674-9871/© 2018, China University of Geosciences (Beijing) and Peking University. Production and hosting by Elsevier B.V. This is an open access article under the CC BY-NC-ND license (http://creativecommons.org/licenses/by-nc-nd/4.0/).

Table 1
Average shale and greywacke composition (in wt.%) from the Archean, Phanerozoic, and Proterozoic after Condie (1993).

Lithology	Shale			Greywacke		
Age	Archean	Prot.	Phan.	Archean	Prot.	Phan.
SiO_2	60.9	63.1	63.6	66.1	65.4	66.3
TiO_2	0.6	0.6	0.8	0.6	0.7	0.7
Al_2O_3	17.5	17.5	17.8	15.3	15.5	15.5
FeO^T	7.5	5.7	5.9	5.5	6.1	6.2
MgO	3.9	2.2	2.3	3.5	2.2	2
CaO	0.6	0.7	1.3	2.5	2.5	3.2
Na_2O	0.7	1.1	1.1	2.9	3	3.1
K_2O	3.1	3.6	3.8	2	2.4	2.3
P_2O_5	0.1	0.12	0.14	0.12	0.15	0.14
Mg#	0.34	0.28	0.28	0.39	0.27	0.24
A/CNK	2.4	1.9	1.8	1.4	1.3	1.2

Mg# = Mg/(Mg + FeO); A/CNK = Al/(Ca + Na + K).

Although this study is based on the secular change in shale and greywacke compositions, the timing of metamorphism of these sedimentary rocks is not strictly relevant and we recognize that Archean compositions may have been metamorphosed and/or reworked through Proterozoic and Phanerozoic orogenesis. However, average Archean compositions were determined using rocks from terrains with little to none Phanerozoic and Proterozoic overprint (Condie, 1993). We investigated the influence of rock composition on water retention in hydrous minerals below solidus temperatures and the chemistry and degree of melt generated at suprasolidus temperatures in water-absent conditions.

2. Starting material

To investigate secular changes in sediment fertility, partial melting and the nature of the generated magma, we used averaged shale and greywacke compositions from the Archean, Proterozoic and Phanerozoic eons (Table 1; Condie, 1993). The shale compositions represent a global average of shales sampled from cratonic and passive margin successions. The greywacke compositions were assembled from turbidite units within Precambrian greenstone belt and modern volcanic arcs. Archean shales are characterized by a low K content (3.1 wt.%) and a high Mg# (Mg# = Mg/[Mg + FeO^t]) and A/CNK values (A/CNK = Al/(Ca + Na + K)) of 0.34 and 2.4, respectively (Condie, 1993). Proterozoic and Phanerozoic shales contain higher concentrations of K, 3.6–3.8 wt.%, and lower Mg# and A/CNK values of 0.28 and 1.8–1.9, respectively. Apart from a decrease in Mg# from 0.39 to 0.24, the major element composition of greywacke does not vary significantly through time (McLennan, 1982; Condie, 1993). The most significant secular change in greywacke compositions are found in their trace elements compositions (McLennan and Taylor, 1991), and as such are not likely to exert much control on the primary mineral assemblage.

3. Model setup

Phase equilibria of greywacke and shale from the Archean, Proterozoic and Phanerozoic were modelled using version 6.7.5 of the Perple_X software package (Connolly, 2009) in the system MnO–Na_2O–CaO–K_2O–FeO–MgO–Al_2O_3–SiO_2–H_2O–TiO_2–O_2 (MnNCKFMASHTO). For all calculations, we used the 2004 update of the Holland and Powell (1998) thermodynamic database (http://www.perplex.ethz.ch/). This approach assumes equilibrium is maintained between phases across the chosen range of pressures and temperatures (Connolly and Kerrick, 1987; Connolly, 1990). Solution models used are as follows: silicate melt model after Green et al. (2016); feldspar (Fuhrman and Lindsley, 1988); chlorite (Holland et al., 1998); amphibole model after Diener and Powell (2012); white mica (Coggon and Holland, 2002; Auzanneau et al., 2010); ilmenite (White et al., 2000); hydrous cordierite (Holland and Powell, 1998); orthopyroxene (White et al., 2001); biotite (White et al., 2007); and garnet (White et al., 2014). Mineral abbreviations follow Kretz (1983). To investigate the maximum amount of water that shale and greywacke compositions retain under subsolidus pressure and temperature conditions, fluid was considered in excess and treated as a pure H_2O. Adding CO_2 would lower a_{H2O} and reduce the stability of hydrous phases, resulting in a reduction of muscovite, biotite, and chlorite at higher temperatures. As such, maximum water retention values were obtained by summing the water content in the different hydrous phases. For modelling of suprasolidus conditions, bulk-rock fluid contents were individually fixed to be minimally saturated (<0.5 mol.% of free H_2O) at the point at which the relevant geotherm intersects the solidus. As the focus of this paper is on the metamorphism of siliciclastic metasedimentary compositions in a continental collisional setting, we investigated the modal proportion of hydrous minerals along two Barrovian-type geotherms from 400 to 1000 °C. The two geotherms correspond to the upper and lower bounds of orogenic thermal gradients compiled by Brown (2006) in a global review of peak metamorphic conditions from Archean to Phanerozoic terrains. The lower pressure geotherm (A) was set at 1330 °C/GPa intersecting the solidus at ~675 °C and 0.5 GPa. The higher pressure geotherm (B) was set at 800 °C/GPa, which intersects the solidus at ~675 °C and 0.8 GPa. Along both geotherms, we investigate how secular compositional variations effect the chemistry and modal proportion of silicate melt.

4. Results

4.1. Subsolidus mineral-bound water

The retention of water in metasedimentary rocks that have undergone compaction, diagenesis and low-grade metamorphism is primarily a function of the stability of hydrous minerals (Walther and Orville, 1982). At lower greenschist facies metamorphic conditions (400 °C) shales and greywackes can respectively retain up to 4.5 wt.% and 3 wt.% mineral-bound water, respectively (Fig. 1). As temperature increases these minerals devolatilize. The temperature and pressure at which devolitization occurs is strongly influenced by the equilibria conditions of the following three continuous reactions (Ramsay, 1973; Ahn and Nakamura, 2000):

$$Chl + Ms^1 + Ilm = Bt + Ms^2 + H_2O \pm Qtz \quad (1)$$

$$Ms + Qtz + Chl = Al_2SiO_5 + Bt + H_2O \quad (2)$$

$$Ms + Qtz = Al_2SiO_5 + Kfs + H_2O \quad (3)$$

Accordingly, the temperature at which geotherms A and B intersect the assemblage field boundaries is markedly different for the different shale and greywacke compositions (Fig. 1). The higher Fe+Mg content of Archean shale and greywacke results in a greater volume of chlorite, and corresponding mineral-bound water, up until chlorite breakdown at 550–600 °C (Fig. 1) (for phase proportion along the two geotherms, see Supplementary Fig. S1). Along the higher pressure geotherm (B), Archean shale retains up to ~4 wt.% water to lower-crustal pressures of 0.75 GPa, twice that of Phanerozoic shale under the same conditions. In Archean shale, the maximum bulk-water content along the higher pressure geotherm (B) drops from 3.8 wt.% to 1.5 wt.% over a temperature window of 590–600 °C. By contrast, Proterozoic and Phanerozoic shale compositions undergo two major devolatilization events along

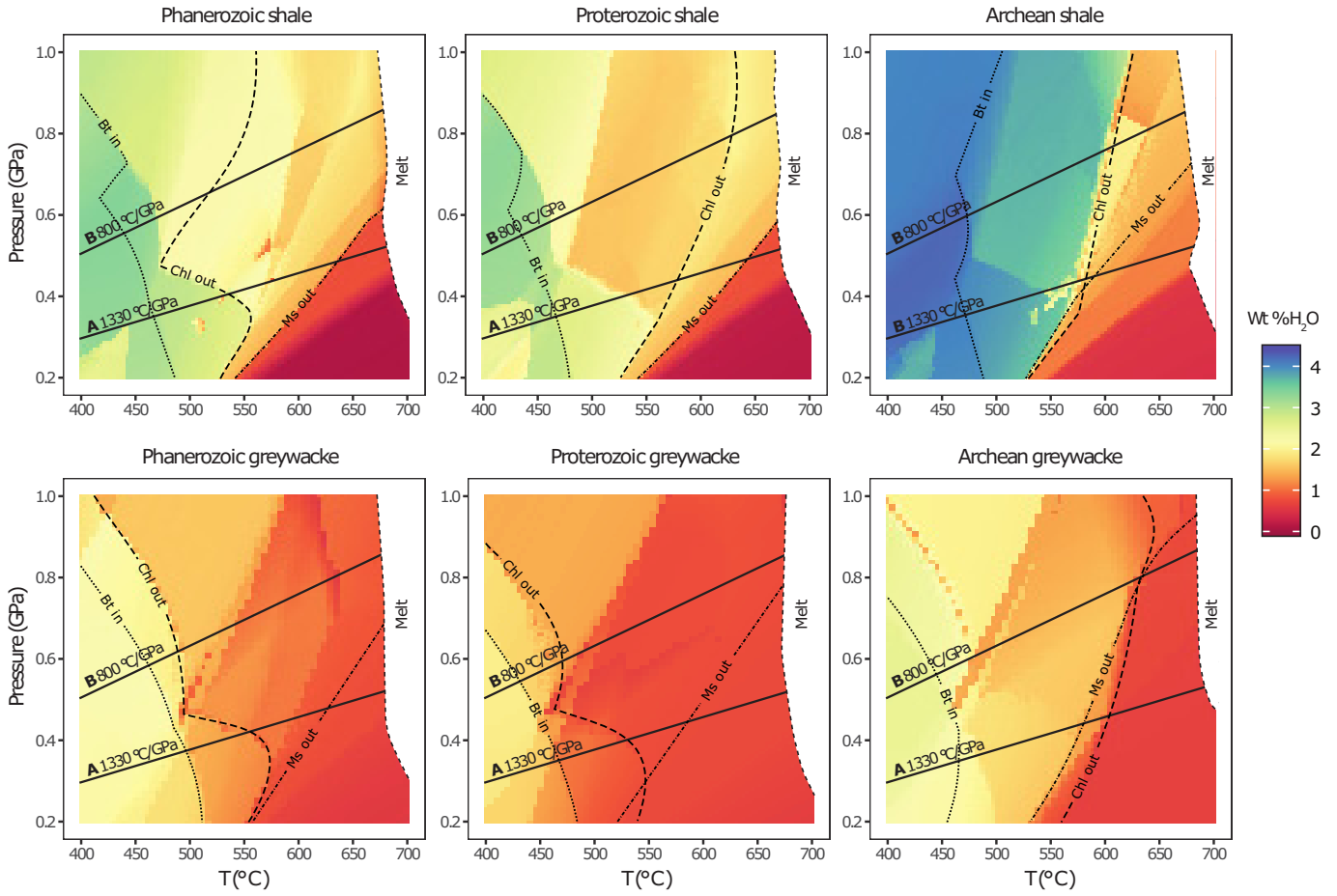

Figure 1. Heatmaps showing maximum mineral-bound H_2O content (wt.%) for Phanerozoic, Proterozoic, and Archean shale and greywacke.

geotherm (B) at ~475 °C with the initial breakdown of chlorite, and over a temperature range of 600–625 °C when chlorite is fully consumed. The amount of water removed from the stable mineral assemblage over the two stages of devolatilization in the Proterozoic and Phanerozoic shales is ~1 wt.% and ~0.5 wt.%, respectively. The secular change in mineral-bound water of greywacke is less pronounced, although a similar trend of increased water content in the older compositions is observed. As with the shale compositions, the stability of chlorite at higher temperatures in Archean greywacke may enable greater amount of mineral-bound water to be held in metamorphosed sedimentary margins.

4.2. Mineral-bound water content at $T_{solidus}$

The amount of mineral-bound water stable immediately below the water-saturated solidus temperature ($T_{solidus}$) is an important measure of the ability of metasedimentary rocks to retain water to lower crustal conditions. The variation observed in the modelled compositions mirrors changes in the modal amount of chlorite, muscovite, and biotite, and is dependent on both pressure and bulk composition (Fig. 1). At the lower pressure $T_{solidus}$ of geotherm (A), mineral-bound water in Archean to Phanerozoic shale varies from 1.1 wt.% to 0.8 wt. % (Table 2). This trend is reversed along the higher pressure geotherm (B), where mineral-bound water at $T_{solidus}$ in Archean to Phanerozoic shale varies from 1.4 wt.% to 1.8 wt.% (Table 2). The total amount of water lost in Archean shale by the time it reaches $T_{solidus}$ is ~3 vol.% of the total rock volume for both geotherms, whereas Proterozoic shales (1.7–2.5 vol.%) and Phanerozoic shales (1.4–1.7 vol.%) are less affected by this phenomenon (Fig. 2). In contrast to the trend observed in the shales, the maximum amount of mineral-bound water in the greywacke compositions at $T_{solidus}$ shows little variation.

Table 2
Maximum H_2O content (in wt.%) for water-saturated solidus along two geotherms A (1330 °C/GPa) and B (800 °C/GPa).

Sediment	Shale			Greywacke		
Eon	Archean	Proterozoic	Phanerozoic	Archean	Proterozoic	Phanerozoic
H_2O^A	1.1	0.8	0.8	0.7	0.8	0.7
H_2O^B	1.4	1.7	1.8	0.7	0.6	0.5
$T^A_{solidus}$	729	715	715	765	719	722
$T^B_{solidus}$	680	680	680	736	719	712

$T_{solidus}$ in degrees centigrade.

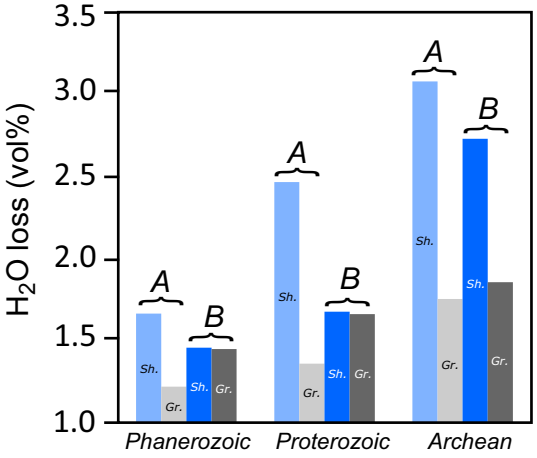

Figure 2. Total H_2O loss during devolatilization from 400 °C to $T_{solidus}$ for geotherms A and B. Sh–Shales, Gr–Greywackes.

4.3. Shale and greywacke melt-fertility

In the absence of a metamorphic fluid with high a_{H_2O} in quartz-bearing rocks, melt-fertility (i.e. the amount of melt that can be generated in a rock at given metamorphic conditions) is primarily controlled by the modal proportion of hydrous minerals stable when the rock reaches the equilibria conditions of water-absent melting (Thompson and Algor, 1977; Brown, 2007). Since the position of the individual water-absent melting curves varies with bulk composition (Table 2; Douce, 1996), we first present the proportions of the hydrous phases that are stable where geotherm A and B intersect the water-saturated solidus ($T_{solidus}$), then discuss the absolute vol.% of melt generated in each composition. Along the lower pressure geotherm(A), muscovite is absent in all shale and greywacke compositions and biotite is predicted to be the key hydrous phase (Fig. 3). Under water-saturated conditions,up to 30 vol.% cordierite is stable where geotherm A intersects $T_{solidus}$ of the Archean shale composition. At the increased pressure where geotherm B intersects $T_{solidus}$ there is not able variation in the volume ratio of biotite/muscovite, from a ratio of 4.4 in the Archean shale composition to ratios of 0.5 and 0.4 in the Proterozoic and Phanerozoic respectively (Fig. 3). Accordingly, water-absent biotite melting is predicted to play a far greater role in the generation of melt in Archean-aged shale, and water-absent muscovite melting is of greater importance in Proterozoic- and Phanerozoic-aged shale. In greywacke, the total volume of hydrous minerals is lower than in shale, and both muscovite and cordierite play only a minor role in the generation of melt. Consequently, regardless of the age of the sediment, the partial melting of metamorphosed greywacke is mainly controlled by water-absent biotite melting.

A consequence of the increased stability of muscovite at depth is that up to 25 vol.% melt may be generated by water-absent muscovite dehydration melting in shale along the higher pressure geotherm (B). However, there is a notable difference in the volume of melt generated by muscovite dehydration among the different shale compositions (Fig. 4). Archean shale is predicted to produce <10 vol.% melt by muscovite dehydration melting. Whereas, Proterozoic and Phanerozoic shale is predicted to generate ~20 vol.% and ~25 vol.% melt, respectively. The secular disparity in the melt fertility of shale extends to temperatures in excess of 1000 °C, where the total volume of melt generated by Phanerozoic shale is approximately 40% greater than that generated in Archean shale. One important consequence of the increased stability of muscovite at depth is that the predicted volume of melt generated along the higher pressure geotherm (B) at temperatures below 800 °C, typical

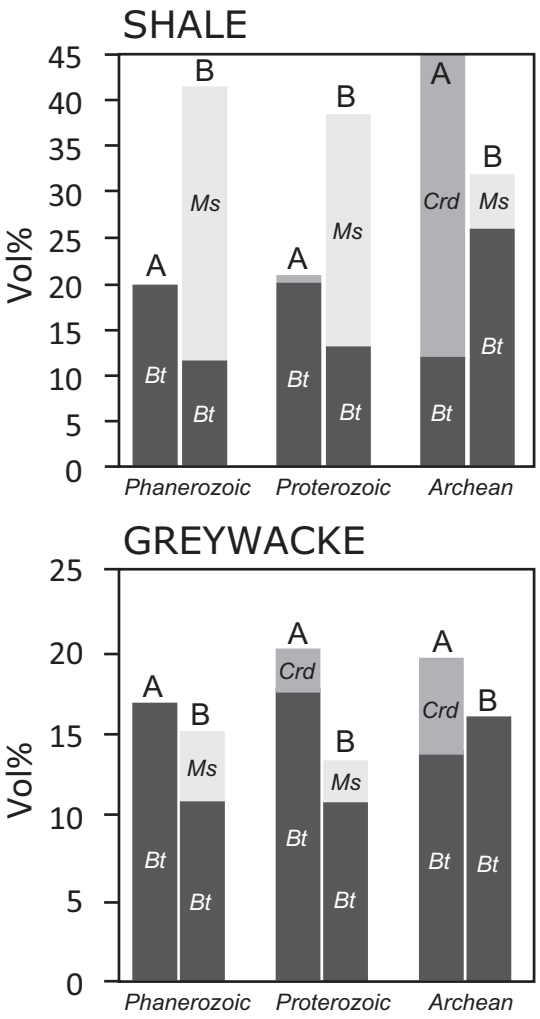

Figure 3. Volume % of hydrous phases at $T_{solidus}$ for the different shale and greywacke along geotherms A and B. Bt: biotite; Ms: muscovite; Crd: cordierite.

of most orogenic settings, is greater than the amount of melt generated along the lower pressure geotherm (A). Under the same conditions, greywacke exhibits the opposite trend with more voluminous melting occurring for geotherm (A) (Fig. 4).

4.4. Melt chemistry and viscosity

While temperature will have a first-order control on the ferromagnesian content of metasedimentary derived partial melts (Brown and Fyfe, 1970), the amount of Ca in the melt predominately varies with changes in the composition of the melt source (Fig. 5). The effect of a secular change in shale compositions on the Ca content of melt is greatest for geotherm B (Fig. 4). The calculations presented here suggest that the partial melting of shale and greywacke will produce melt with a narrow range of SiO_2 content (A: 68–70 wt.%; B: 63–67 wt.%; Supplementary Table S1). For both geotherms, the lack of significant secular variation in the Ca content in the greywackes results in similar melt compositions among Archean, Proterozoic and Phanerozoic greywackes (Fig. 5).

Within the set of calculation done for each geotherm, the bulk water content of melts derived from the different shale compositions does not show significant variation.

There is, however, notable variation in the bulk water content of the melt generated by shale between the two geotherms. Initial

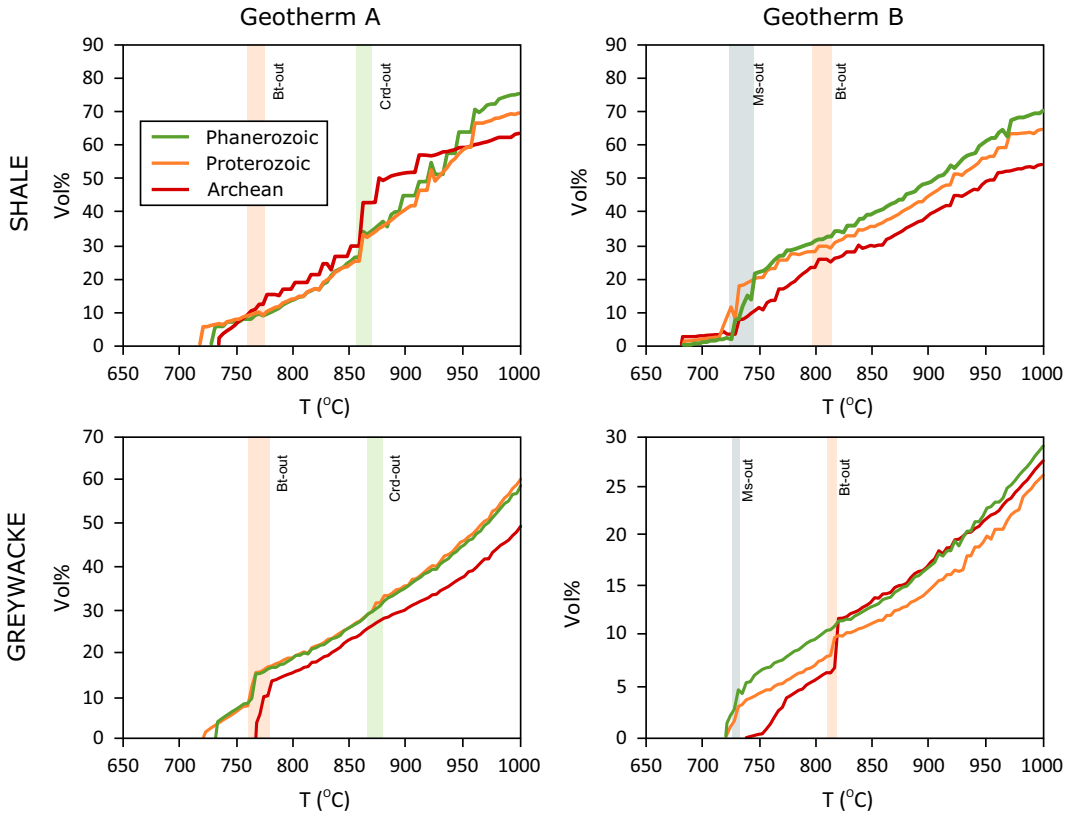

Figure 4. Modal proportion of melt along geotherms A and B for shales and greywackes under water saturated solidus (see H_2O values in Table 2). Vertical boxes indicate the disappearance of hydrous phases (Bt: biotite; Ms: muscovite; Crd: cordierite).

melting at $T_{solidus}$ of geotherm A results in a melt that contains ~7–8 wt.% H_2O. As temperatures increase to 1000 °C, the melt water content drops to ~1–2 wt.% H_2O (Supplementary Table S1). By contrast, the water content of melt generated at $T_{solidus}$ of geotherm B is ~12–13 wt.% H_2O, dropping to ~3 wt.% H_2O at 1000 °C (Supplementary Table S1).

Melt viscosity (η) is influenced by temperature and the melt water content (Clemens and Petford, 1999). Accordingly, melt viscosity varies most significantly between geotherm A and B rather than amongst the different shale compositions. Between $T_{solidus}$ and 1000 °C of geotherm A, melt viscosity increases from 10^4 Pa s to 10^7 Pa s. Whereas, a lower range in melt viscosities from 10^1 Pa s to 10^6 Pa s is predicted between $T_{solidus}$ and 1000 °C of geotherm B.

The calculations of melt water content and viscosity in the greywacke scenarios show a similar trend as described for shale. The predicted melt water content between $T_{solidus}$ and 1000 °C along geotherm A (~8–1 wt.% H_2O) is lower than along geotherm B (~10–3 wt.% H_2O). As a result, the viscosity of melt generated along the lower-pressure geotherm A is slightly lower than along geotherm B, 10^4–10^7 Pa s and 10^2–10^6 Pa s respectively.

5. Discussion

5.1. The retention of water in siliciclastic continental margins

Biotite, muscovite, and chlorite contain the majority of the water that is held in metamorphosed siliciclastic rocks, with an average of 3.8 wt.%, 4.5 wt.%, and 11 wt.% of water respectively. Consequently, chlorite has the greatest potential to transport water to the middle and lower crust. The increased stability of chlorite in the more ferromagnesic Archean shale and greywacke compositions suggests that Archean orogenic belts retain a greater proportion of water than Proterozoic and Phanerozoic equivalents. The nearly two-fold increase in the amount of water held in Archean shale compared to Phanerozoic shale at middle–lower crustal conditions suggests that the role of siliciclastic sediments in the sequestration and retention of mineral-bound crustal water has decreased significantly through Earth's history. While the end of the Archean is characterized by the progressive emergence of modern subduction processes (Fischer and Gerya, 2016) and continental freeboard studies (i.e. average sea level surface relative to the continents) indicate that global sea level has fluctuated by <500 m over the past ca. 3 Ga (Galer, 1991; Eriksson, 1999), the secular change in the hydration state of continental margins is likely of second order importance to the global water cycle (Poli and Schmidt, 1995; Parai and Mukhopadhyay, 2012). However, there are still several important implications to this finding. The more water-rich Archean shale would be an important source of metamorphic fluid in the middle and lower crust. Since metamorphic water is the limiting reactant in most retrograde reactions (e.g. Haack and Zimmermann, 1996) and a powerful catalyst for both chemical and microstructural change (Ague, 1991), the structurally higher levels of Archean siliciclastic continental margins are expected to display greenschists facies mineral assemblages. Similarly, by virtue of the increased amount of water released at depth by the breakdown of chlorite, our results suggest that there may have been a greater capacity for metamorphic fluids to redistribute soluble components across crustal levels in the Archean.

5.2. Changes in water flux and mineralization

The release of water by the breakdown of hydrous minerals during prograde heating and decompression raises the issue of fluid circulation in the middle and lower crust and how it might

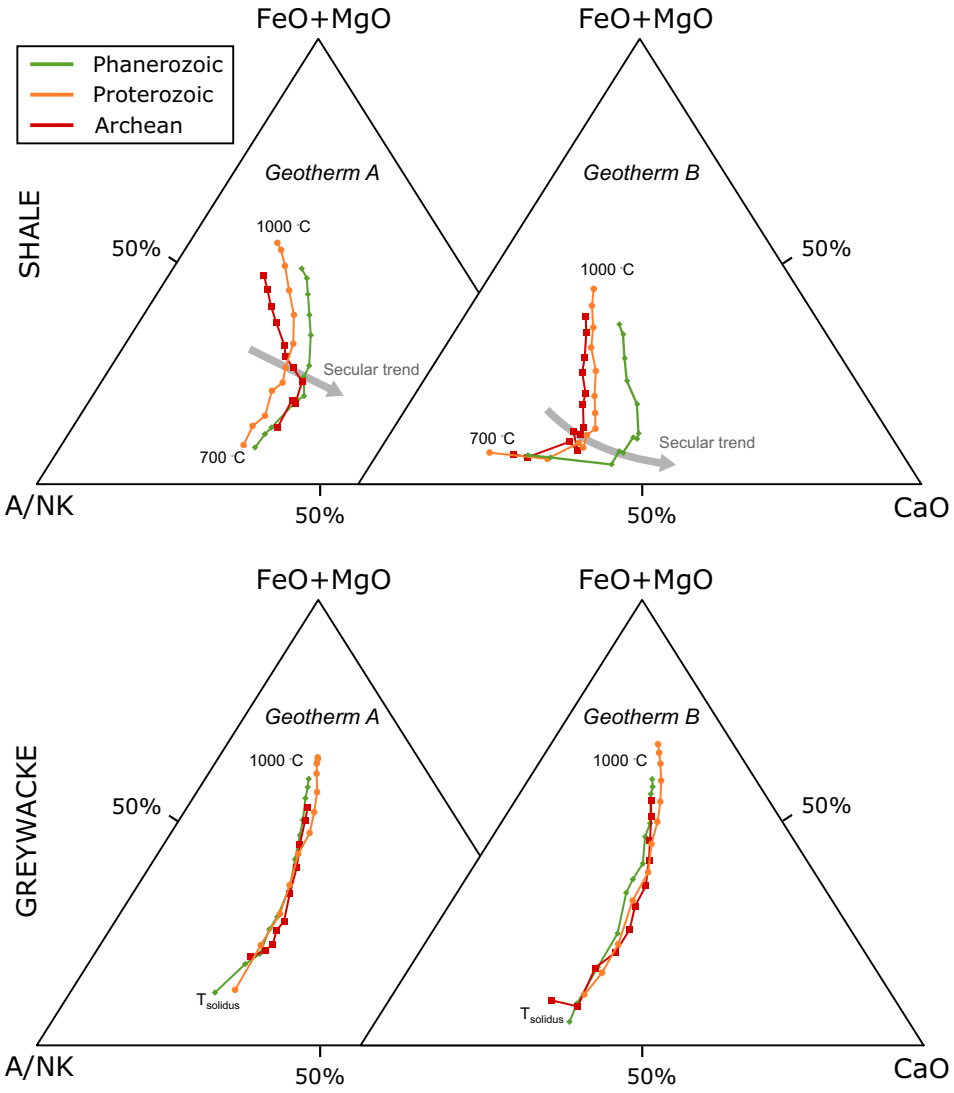

Figure 5. Evolution of melt chemistry generated by water-absent partial melting of shale and greywacke along geotherm A and B between $T_{solidus}$ and 1000 °C. A/NK = Al_2O_3/(Na_2O + K_2O).

affect the surrounding lithologies. The results presented here indicate that by the time water-absent partial melting occurs, the shale and greywacke compositions have lost a minimum of 60% of their initial mineral-bound water. As summarised in Fig. 2, a greater total volume of water is released during heating along the lower pressure geotherm (A). One limitation of the models presented here is that dehydration was only considered along a linear *P*–*T* path and so the role of exhumation in the production of metamorphic water was not considered. As demonstrated by Vry et al. (2010), the exhumation of hydrous minerals from mid-crustal conditions plays and important role in further dehydrating siliciclastic rocks. However, exhumation of the more hydrous Archean siliciclastic material at temperatures below the solidus would result in a further release of mineral-bound water, exaggerating the effect of secular compositional changes. The effects of decompression notwithstanding, there is a notable secular change in the degree and conditions under which siliciclastic rocks dehydrate. Archean shale is predicted to experience a significant dehydration over a narrow temperature window of ~550–580 °C corresponding to the breakdown of chlorite.

The breakdown of mica at depth is expected to contribute to an increase in fluid pressure and the extraction of water to higher structural levels in the crust (Walther and Orville, 1982; Yardley, 1983; Connolly, 1997). If the extraction remains channelized, metamorphic fluid pathways are expected to maintain high fluid-rock ratios potentially resulting in the formation of quartz veins in the upper and middle crust (Walther and Orville, 1982; Yardley, 1983).

The relatively higher potential for Archean shale to dehydrate and drive fluid release may be an important consideration in the formation of gold mineralized quartz veins in Precambrian metamorphic terrains (Robert and Brown, 1986; Groves et al., 1987; Kerrich and Feng, 1992; Robert et al., 1995; Jia and Kerrich, 2000). While preservation potential and exposure levels must be considered, the decrease in shale hydration potential through time showed in this study (Fig. 6) correlates with the progressive decrease in the global amount of orogenic gold resources (Goldfarb et al., 2001). Most of the worlds orogenic gold deposits are found within Archean cratons (3.0–2.5 Ga). Reworked metamorphic and placer gold deposits appear to be largely concentrated in

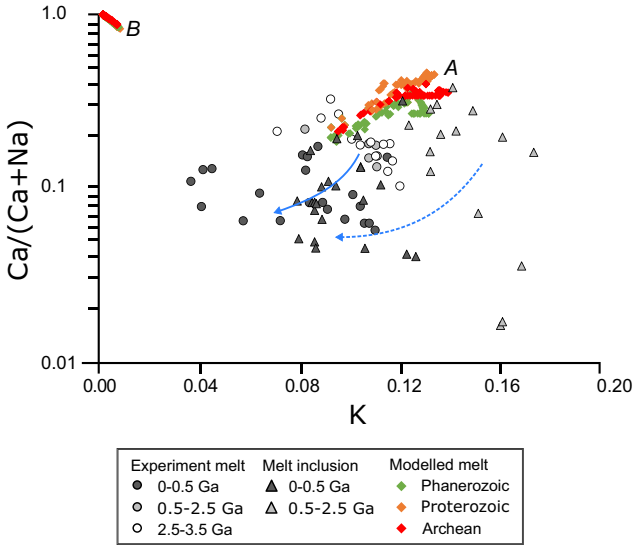

Figure 6. Melt inclusion and experimental melt chemistries and compared with modelled melts (in moles). The plain arrow indicates secular changes in the experimental melt composition. Compilation of melt compositions from Acosta-Vigil et al. (2001), Bartoli et al.(2013), Ferrero et al. (2012, 2014). A: lower-pressure geotherm; B: higher-pressure geotherm.

Proterozoic terrains (1.8–0.6 Ga), while there are no known gold deposits younger than 50 Ma (Goldfarb et al., 2001).

5.3. Implications of secular changes in siliciclastic compositions on the observable mineral assemblages in metamorphosed continental margins

The predicted increase in chlorite stability with ferromagnesic content maps on to the observed prevalence of chlorite-rich lithologies in Paleoproterozoic and Archean siliciclastic terrains (e.g. Dunbar and McCall, 1971; de Wit, 1991; Macfarlane et al., 1994; Hunter et al., 1998; Komiya et al., 1999; Sharpe and Gemmell, 2002; Saito et al., 2015). The relatively high abundance of chlorite in Archean shale, compared to the younger shale compositions, contributes to the 'greenstone' denomination of Archean metasedimentary units. Archean greenstone belts are successions of supracrustal rocks, largely comprised of mafic volcanics, turbidites and clastic sediments metamorphosed under greenschist to amphibolite facies conditions (Condie, 1981). While the definition of greenstone belt might be extended to younger terranes as suggested by Condie (1981), this study demonstrates the compositional sensitivity of chlorite in shale. Under lower-amphibolite facies conditions Archean shale compositions produce a chlorite schist, whereas under the same conditions Proterozoic and Phanerozoic compositions form a muscovite-biotite schist. We highlight this predicted mineral assemblage variation to show the care with which the modern-day metamorphic facies system must be applied to Archean compositions.

5.4. Evolution of silicate melts

In continental collision settings, the onset of partial melting typically occurs under upper-amphibolite facies conditions (Sawyer et al., 2011). Under water-poor conditions, major melt production in metasedimentary rocks generally proceeds at temperatures above 700 °C by incongruent melting of micas to produce peraluminous granitic melts (Douce and Harris, 1998). The composition of the melt generated is dependent on the mineral assemblage of the protolith (e.g. hydrous phases) and the degree of partial melting (Stevens et al., 1997, 2007; Douce and McCarthy, 1998; Clemens et al., 2011; Clemens and Stevens, 2012). The proportion of hydrous minerals stable at suprasolidus temperatures is therefore a key parameter when considering the composition of partial melt. Owing to the increased stability of chlorite, the more mafic Archean shale undergoes a larger degree of subsolidus dehydration, which lowers its potential to generate melt at temperatures below 900 °C. Additionally, the higher iron and magnesium content of Archean shale favours the formation of biotite over muscovite at temperatures above 550 °C. At higher pressures, with the increasing dominance of water-absent muscovite dehydration melting, a larger volume of H_2O-rich meltis generated (Fig. 4). Our calculations suggest that the generation of relatively water-rich peraluminous melt of leucogranitic composition has increased from the Archean to Phanerozoic.

The production of anatectic melts and the genesis of S-type granite (i.e. final product of the partial melting of sedimentary source), has been demonstrated to involve a large set processes such as disequilibrium partial melting (e.g. Taylor et al., 2014; Guevara and Caddick, 2016; Nicoli et al., 2017) and entrainment of peritectic phases (Stevens et al., 2007; Garcia-Arias and Stevens, 2017a,b), which are not considered here. Therefore, comparing the modelled melts with a possible secular evolution of S-type granite chemistry (Clemens and Stevens, 2012) is a complex task and beyond the scope of this paper. The modelled melt compositions are more likely to mimic melt inclusion chemistries from anatectic terrains (Acosta-Vigil et al., 2001; Ferrero et al., 2012, 2014; Bartoli et al., 2013) and experimental melts designed to reproduce partial melting of a pelitic sources of Precambrian and Phanerozoic compositions (Stevens et al., 1997; Douce and Harris, 1998; Pickering and Johnston, 1998) (Fig. 6). Melt inclusion data from Archean terrains is scarce, however, Proterozoic and Phanerozoic melt inclusion compositions define a secular trend with a decrease in K content and Ca:Na ratio through time (Fig. 6). Experimental melts follow a similar pattern (Fig. 6). The melt compositions modelled in our study best reproduce the general trends seen in the melt inclusion and experimental data for the lower pressure geotherm A (Fig. 6). However, further careful consideration of the uncertainties introduced during the selection of effective bulk compositions (Palin et al., 2016) are required to rigorously compare modelled results with natural data.

6. Conclusions

This study demonstrates the strength of thermodynamic modelling in exploring the metamorphic consequences of a secular changes in Earth's crust. We designed this study to investigate ideal scenarios of sediment burial during an orogenic episode. Accordingly, it does not reproduce a specific situation but rather emphasises the general variations that may be expected to result from changes in shale and greywacke compositions.

The key findings of this study are:

(1) Changes in shale (and to a lesser extend greywacke) composition through time directly affect the abundance of hydrous phases in the equilibrium mineral assemblage. In Archean shales, chlorite is the main hydrous phase at temperatures < 550 °C, which allows the rock to retain up to 4 vol.% of water during the early stage of Barrovian metamorphism.
(2) The ferromagnesium content of shale and greywacke strongly influences the temperature of mica breakdown. Archean shale dehydrates over a narrow temperature window of ~550–580 °C corresponding to the breakdown of chlorite whereas, Proterozoic and Phanerozoic shale compositions undergo two major dehydration events at ~475 °C and 600–625 °C.

(3) Partial melting of Archean shales is controlled by the dehydration of biotite while water-absent muscovite dehydration melting is the primary melt producing reaction in Proterozoic and Phanerozoic shale and greywacke.
(4) Secular change in the compositions of shale and greywacke is reflected in the evolution of anatectic melt towards an increasingly less viscous, Ca-rich, and Mg-poor monzogranite.

Acknowledgements

The authors thank Richard Palin and Christopher J. Spencer, for their invitation to join this special issue. Victor Guevara and an anonymous reviewer are thanked for providing useful comments that improved this study.

Appendix A. Supplementary data

Supplementary data related to this article can be found at https://doi.org/10.1016/j.gsf.2017.12.009.

References

Acosta-Vigil, A., Pereira, M.D., Shaw, D.M., London, D., 2001. Contrasting behaviour of boron during crustal anatexis. Lithos 56 (1), 15–31.
Ague, J., 1991. Evidence for major mass transfer and volume strain during regional metamorphism of pelites. Geology 19, 855–858.
Ague, J.J., 2011. Extreme channelization of fluid and the problem of element mobility during Barrovian metamorphism. American Mineralogist 96 (2–3), 333–352.
Ahn, K.S., Nakamura, Y., 2000. The natural reaction muscovite + chlorite + chloritoid = andalusite + biotite + quartz + H_2O and a new petrogenetic grid. Geosciences Journal 4 (1), 25–39.
Auzanneau, E., Schmidt, M.W., Vielzeuf, D., Connolly, J.D., 2010. Titanium in phengite: a geobarometer for high temperature eclogites. Contributions to Mineralogy and Petrology 159 (1), 1.
Barley, M.E., Bekker, A., Krapež, B., 2005. Late Archean to Early Paleoproterozoic global tectonics, environmental change and the rise of atmospheric oxygen. Earth and Planetary Science Letters 238 (1), 156–171.
Bartoli, O., Cesare, B., Poli, S., Bodnar, R.J., Acosta-Vigil, A., Frezzotti, M.L., Meli, S., 2013. Recovering the composition of melt and the fluid regime at the onset of crustal anatexis and S-type granite formation. Geology 41 (2), 115–118.
Brown, G.C., Fyfe, W.S., 1970. The production of granitic melts during ultrametamorphism. Contributions to Mineralogy and Petrology 28 (4), 310–318.
Brown, M., 2006. Duality of thermal regimes is the distinctive characteristic of plate tectonics since the Neoarchean. Geology 34 (11), 961–964.
Brown, M., 2007. Crustal melting and melt extraction, ascent and emplacement in orogens: mechanisms and consequences. Journal of the Geological Society 164 (4), 709–730.
Campbell, I.H., Allen, C.M., 2008. Formation of supercontinents linked to increases in atmospheric oxygen. Nature Geoscience 1 (8), 554–558.
Clemens, J.D., Petford, N., 1999. Granitic melt viscosity and silicic magma dynamics in contrasting tectonic settings. Journal of the Geological Society 156 (6), 1057–1060.
Clemens, J.D., Stevens, G., Farina, F., 2011. The enigmatic sources of I-type granites: the peritectic connexion. Lithos 126 (3), 174–181.
Clemens, J.D., Stevens, G., 2012. What controls chemical variation in granitic magmas? Lithos 134, 317–329.
Clemens, J.D., Vielzeuf, D., 1987. Constraints on melting and magma production in the crust. Earth and Planetary Science Letters 86 (2–4), 287–306.
Coggon, R., Holland, T.J.B., 2002. Mixing properties of phengitic micas and revised garnet-phengitethermobarometers. Journal of Metamorphic Geology 20 (7), 683–696.
Condie, K.C., 1981. Archean Greenstone Belts, vol. 3. Elsevier.
Condie, K.C., 1993. Chemical composition and evolution of the upper continental crust: contrasting results from surface samples and shales. Chemical Geology 104 (1–4), 1–37.
Connolly, J.A.D., 1990. Multivariable phase diagrams: an. algorithm based on generalized thermodynamics. American Journal of Sciences 290, 666–718.
Connolly, J.A.D., 1997. Devolatilization-generated fluid pressure and deformation-propagated fluid flow during prograde regional metamorphism. Journal of Geophysical Research: Solid Earth 102 (B8), 18149–18173.
Connolly, J.A.D., 2009. The geodynamic equation of state: what and how. Geochemistry, Geophysics, Geosystems 10 (10).
Connolly, J.A.D., Kerrick, D.M., 1987. An algorithm and computer program for calculating composition phase diagrams. Calphad 11 (1), 1–55.
Depine, G.V., Andronicos, C.L., Phipps-Morgan, J., 2008. Near-isothermal conditions in the middle and lower crust induced by melt migration. Nature 452 (7183), 80.
de Wit, M.J., 1991. Archaean greenstone belt tectonism and basin development: some insights from the Barberton and Pietersburg greenstone belts, Kaapvaal Craton, South Africa. Journal of African Earth Sciences (and the Middle East) 13 (1), 45–63.
Dhuime, B., Hawkesworth, C.J., Cawood, P.A., Storey, C.D., 2012. A change in the geodynamics of continental growth 3 billion years ago. Science 335 (6074), 1334–1336.
Dhuime, B., Hawkesworth, C.J., Delavault, H., Cawood, P.A., 2017. Continental growth seen through the sedimentary record. Sedimentary Geology 357, 16–32.
Diener, J.F.A., Powell, R., 2012. Revised activity–composition models for clinopyroxene and amphibole. Journal of Metamorphic Geology 30 (2), 131–142.
Douce, A.E.P., 1996. Effects of pressure and H_2O content on the compositions of primary crustal melts. Earth and Environmental Science Transactions of the Royal Society of Edinburgh 87 (1–2), 11–21.
Douce, A.E.P., Harris, N., 1998. Experimental constraints on Himalayan anatexis. Journal of Petrology 39 (4), 689–710.
Douce, A.E.P., Johnston, A.D., 1991. Phase equilibria and melt productivity in the pelitic system: implications for the origin of peraluminous granitoids and aluminous granulites. Contributions to Mineralogy and Petrology 107 (2), 202–218.
Douce, A.E.P., McCarthy, T.C., 1998. Melting of crustal rocks during continental collision and subduction. In: When Continents Collide: Geodynamics and Geochemistry of Ultrahigh-pressure Rocks. Springer, Netherlands, pp. 27–55.
Dunbar, G.J., McCall, G.J.H., 1971. Archaean turbidites and banded ironstones of the Mt. Belches area (Western Australia). Sedimentary Geology 5 (2), 93101–97133.
Dyck, B., Reno, B.L., Kokfelt, T.F., 2015. The majorqaq belt: a record of neoarchaeanorogenesis during final assembly of the north Atlantic craton, southern west Greenland. Lithos 220, 253–271.
Engel, A.E., Itson, S.P., Engel, C.G., Stickney, D.M., Cray, E.J., 1974. Crustal evolution and global tectonics: a petrogenic view. The Geological Society of America Bulletin 85 (6), 843–858.
Eriksson, P.G., 1999. Sea level changes and the continental freeboard concept: general principles and application to the Precambrian. Precambrian Research 97 (3), 143–154.
Ferrero, S., Bartoli, O., Cesare, B., Salvioli-Mariani, E., Acosta-Vigil, A., Cavallo, A., Battiston, S., 2012. Microstructures of melt inclusions in anatectic metasedimentary rocks. Journal of Metamorphic Geology 30 (3), 303–322.
Ferrero, S., Braga, R., Berkesi, M., Cesare, B., LaridhiOuazaa, N., 2014. Production of metaluminous melt during fluid-present anatexis: an example from the Maghrebian basement, La Galite Archipelago, central Mediterranean. Journal of Metamorphic Geology 32 (2), 209–225.
Fischer, R., Gerya, T., 2016. Regimes of subduction and lithospheric dynamics in the Precambrian: 3D thermomechanical modelling. Gondwana Research 37, 53–70.
Flament, N., Gurnis, M., Müller, R.D., 2013. A review of observations and models of dynamic topography. Lithosphere 5 (2), 189–210.
Fuhrman, M.L., Lindsley, D.H., 1988. Ternary-feldspar modeling and thermometry. American Mineralogist 73, 201–215.
Galer, S.J.G., 1991. Interrelationships between continental freeboard, tectonics and mantle temperature. Earth and Planetary Science Letters 105 (1–3), 214–228.
Garcia-Arias, M., Stevens, G., 2017a. Phase equilibrium modelling of granite magma petrogenesis: a. An evaluation of the magma compositions produced by crystal entrainment in the source. Lithos 277, 131–153.
Garcia-Arias, M., Stevens, G., 2017b. Phase equilibrium modelling of granite magma petrogenesis: B. An evaluation of the magma compositions that result from fractional crystallization. Lithos 277, 109–130.
Goldfarb, R.J., Groves, D.I., Gardoll, S., 2001. Orogenic gold and geologic time: a global synthesis. Ore Geology Reviews 18 (1), 1–75.
Green, E.C.R., White, R.W., Diener, J.F.A., Powell, R., Holland, T.J.B., Palin, R.M., 2016. Activity–composition relations for the calculation of partial melting equilibria in metabasic rocks. Journal of Metamorphic Geology 34 (9), 845–869.
Groves, D.I., Phillips, G.N., Ho, S.E., Houstoun, S.M., Standing, C.A., 1987. Craton-scale distribution of Archean greenstone gold deposits; predictive capacity of the metamorphic model. Economic Geology 82 (8), 2045–2058.
Guevara, V.E., Caddick, M.J., 2016. Shooting at a moving target: phase equilibria modelling of high-temperature metamorphism. Journal of Metamorphic Geology 34 (3), 209–235.
Haack, U.K., Zimmermann, H.D., 1996. Retrograde mineral reactions: a heat source in the continental crust? Geologische Rundschau 85 (1), 130–137.
Holland, T., Baker, J., Powell, R., 1998. Mixing properties and activity-composition relationships of chlorites in the system MgO-FeO-Al_2O_3-SiO_2-H_2O. European Journal of Mineralogy 395–406.
Holland, T.J.B., Powell, R., 1998. An internally consistent thermodynamic data set for phases of petrological interest. Journal of Metamorphic Geology 16 (3), 309–343.
Hunter, M.A., Bickle, M.J., Nisbet, E.G., Martin, A., Chapman, H.J., 1998. Continental extensional setting for the Archean Belingwe greenstone belt, Zimbabwe. Geology 26 (10), 883–886.
Jia, Y., Kerrich, R., 2000. Giant quartz vein systems in accretionary orogenic belts: the evidence for a metamorphic fluid origin from δ 15 N and δ 13 C studies. Earth and Planetary Science Letters 184 (1), 211–224.
Johnsson, M.J., 1993. The system controlling the composition of clastic sediments. Geological Society of America Special Papers 284, 1–20.
Kerrich, R., Feng, R., 1992. Archean geodynamics and the Abitibi-Pontiac collision: implications for advection of fluids at transpressive collisional boundaries and the origin of giant quartz vein systems. Earth-science Reviews 32 (1), 33–60.

Kretz, R., 1983. Symbols for rock-forming minerals. American Mineralogist 68, 277–279.
Kolb, J., 2008. The role of fluids in partitioning brittle deformation and ductile creep in auriferous shear zones between 500 and 700 C. Tectonophysics 446 (1).
Komiya, T., Maruyama, S., Masuda, T., Nohda, S., Hayashi, M., Okamoto, K., 1999. Plate tectonics at 3.8–3.7 Ga: field evidence from the Isua accretionary complex, southern West Greenland. The Journal of Geology 107 (5), 515–554.
Le Breton, N., Thompson, A.B., 1988. Fluid-absent (dehydration) melting of biotite in metapelites in the early stages of crustal anatexis. Contributions to Mineralogy and Petrology 99 (2), 226–237.
Macfarlane, A.W., Danielson, A., Holland, H.D., 1994. Geology and major and trace element chemistry of late Archean weathering profiles in the Fortescue Group, Western Australia: implications for atmospheric PO_2. Precambrian Research 65 (1–4), 297–317.
McLennan, S.M., 1982. On the geochemical evolution of sedimentary rocks. Chemical Geology 37 (3–4), 335–350.
McLennan, S.M., Taylor, S.R., 1991. Sedimentary rocks and crustal evolution: tectonic setting and secular trends. The Journal of Geology 99 (1), 1–21.
McLennan, S.M., 2001. Relationships between the trace element composition of sedimentary rocks and upper continental crust. Geochemistry, Geophysics, Geosystems 2 (4).
Nicoli, G., Moyen, J.F., Stevens, G., 2016. Diversity of burial rates in convergent settings decreased as Earth aged. Scientific Reports 6.
Nicoli, G., Stevens, G., Moyen, J.F., Vezinet, A., Mayne, M., 2017. Insights into the complexity of crustal differentiation: K_2O-poor leucosomes within metasedimentary migmatites from the Southern Marginal Zone of the Limpopo Belt, South Africa. Journal of Metamorphic Geology. https://doi.org/10.1111/jmg.12265.
Palin, R.M., Weller, O.M., Waters, D.J., Dyck, B., 2016. Quantifying geological uncertainty in metamorphic phase equilibria modelling; a Monte Carlo assessment and implications for tectonic interpretations. Geoscience Frontiers 7 (4), 591–607.
Palin, R.M., White, R.W., 2016. Emergence of blueschists on Earth linked to secular changes in oceanic crust composition. Nature Geoscience 9 (1), 60.
Parai, R.I.T.A., Mukhopadhyay, S.U.J.O.Y., 2012. How large is the subducted water flux? New constraints on mantle regassing rates. Earth and Planetary Science Letters 317, 396–406.
Poli, S., Schmidt, M.W., 1995. H_2O transport and release in subduction zones: experimental constraints on basaltic and andesitic systems. Journal of Geophysical Research: Solid Earth 100 (B11), 22299–22314.
Pickering, J.M., Johnston, D.A., 1998. Fluid-absent melting behavior of a two-mica metapelite: experimental constraints on the origin of Black Hills granite. Journal of Petrology 39 (10), 1787–1804.
Ramsay, C.R., 1973. The origin of biotite in Archaean meta-sediments near Yellowknife, NWT, Canada. Contributions to Mineralogy and Petrology 42 (1), 43–54.
Robert, F., Brown, A.C., 1986. Archean gold-bearing quartz veins at the Sigma Mine, Abitibi greenstone belt, Quebec; Part I, Geologic relations and formation of the vein system. Economic Geology 81 (3), 578–592.
Robert, F., Boullier, A.M., Firdaous, K., 1995. Gold-quartz veins in metamorphic terranes and their bearing on the role of fluids in faulting. Journal of Geophysical Research: Solid Earth 100 (B7), 12861–12879.
Rudnick, R.L., 1995. Making continental crust. Nature 378 (6557), 571.
Saito, T., Uno, M., Sato, T., Fujisaki, W., Haraguchi, S., Li, Y.B., Maruyama, S., 2015. Geochemistry of accreted metavolcanic rocks from the neoproterozoic Gwna Group of Anglesey–Lleyn, NW Wales, UK: MORB and OIB in the Iapetus Ocean. Tectonophysics 662, 243–255.
Sawyer, E.W., Cesare, B., Brown, M., 2011. When the continental crust melts. Elements 7 (4), 229–234.
Sharpe, R., Gemmell, J.B., 2002. The Archean Cu-Zn magnetite-rich Gossan Hill volcanic-hosted massive sulfide deposit, Western Australia: genesis of a multistage hydrothermal system. Economic Geology 97 (3), 517–539.
Stevens, G., Clemens, J.D., Droop, G.T., 1997. Melt production during granulite-facies anatexis: experimental data from "primitive" metasedimentary protoliths. Contributions to Mineralogy and Petrology 128 (4), 352–370.
Stevens, G., Villaros, A., Moyen, J.F., 2007. Selective peritectic garnet entrainment as the origin of geochemical diversity in S-type granites. Geology 35 (1), 9–12.
Stüwe, K., 1995. Thermal buffering effects at the solidus. Implications for the equilibration of partially melted metamorphic rocks. Tectonophysics 248 (1), 39–51.
Taylor, J., Nicoli, G., Stevens, G., Frei, D., Moyen, J.F., 2014. The processes that control leucosome compositions in metasedimentary granulites: perspectives from the Southern Marginal Zone migmatites, Limpopo Belt, South Africa. Journal of Metamorphic Geology 32 (7), 713–742.
Thompson, A.B., Algor, J.R., 1977. Model systems for anatexis of pelitic rocks. Contributions to Mineralogy and Petrology 63 (3), 247–269.
Veizer, J., Mackenzie, F.T., 2003. Evolution of sedimentary rocks. Treatise on Geochemistry 7, 369–407.
Vry, J., Powell, R., Golden, K.M., Petersen, K., 2010. The role of exhumation in metamorphic dehydration and fluid production. Nature Geoscience 3 (1), 31–35.
Walther, J.V., Orville, P.M., 1982. Volatile production and transport in regional metamorphism. Contributions to Mineralogy and Petrology 79 (3), 252–257.
White, R.W., Powell, R., Holland, T.J.B., 2001. Calculation of partial melting equilibria in the system Na_2O–CaO–K_2O–FeO–MgO–Al_2O_3–SiO_2–H_2O (NCKFMASH). Journal of Metamorphic Geology 19 (2), 139–153.
White, R.W., Powell, R., Holland, T.J.B., 2007. Progress relating to calculation of partial melting equilibria for metapelites. Journal of Metamorphic Geology 25 (5), 511–527.
White, R.W., Powell, R., Holland, T.J.B., Worley, B.A., 2000. The effect of TiO_2 and Fe_2O_3 on metapelitic assemblages at greenschist and amphibolite facies conditions: mineral equilibria calculations in the system K_2O-FeO-MgO-Al_2O_3-SiO_2-H_2O-TiO_2-Fe_2O_3. Journal of Metamorphic Geology 18 (5), 497–512.
White, R.W., Powell, R., Johnson, T.E., 2014. The effect of Mn on mineral stability in metapelites revisited: new a–x relations for manganese-bearing minerals. Journal of Metamorphic Geology 32 (8), 809–828.
Yardley, B.W., 1983. Quartz veins and devolatilization during metamorphism. Journal of the Geological Society 140 (4), 657–663.